Eur. J. Biochem. **269**, 4762–4771 (2002) © FEBS 2002 doi:10.1046/j.1432-1033.2002.03173.x

Role of tyrosine 238 in the active site of *Rhodotorula gracilis* D-amino acid oxidase

A site-directed mutagenesis study

Angelo Boselli, Silvia Sacchi, Viviana Job, Mirella S. Pilone and Loredano Pollegioni

Department of Structural and Functional Biology, University of Insubria, Varese, Italy

Y238, one of the very few conserved residues in the active site of D-amino acid oxidases (DAAO), was mutated to phenylalanine and serine in the enzyme from the yeast *Rhodotorula gracilis*. The mutated proteins are catalytically competent thus eliminating Tyr238 as an active-site acid/base catalyst. Y238F and Y238S mutants exhibit a threefold slower turnover on D-alanine as substrate, which can be attributed to a slower rate of product release relative to the wild-type enzyme (a change of the rate constants for substrate binding was also evident). The Y238 DAAO mutants have spectral properties similar to those of the wild-type enzyme but the degree of stabilization of the flavin semiquinone and the redox properties in the free form of Y238S are different. The binding of the carboxylic acid competitive inhibitors and the substrate D-alanine are changed only slightly, suggesting that the overall substrate binding pocket remains intact. In agreement with data from the pH dependence of ligand binding and with the protein crystal structure, site-directed mutagenesis results emphasize the importance of residue Y238 in controlling access to the active site instead of a role in the substrate/ligand interaction.

Keywords: active site lid; function–structure relationships; flavoprotein; reaction mechanism; substrate recognition.

D-amino acid oxidase (DAAO; EC 1.4.3.3), an FAD-containing flavoprotein, catalyses dehydrogenation of the D-isomer of amino acids to give the corresponding α-imino acids and, after subsequent hydrolysis, α-keto acids and ammonia. The reduced FAD is then reoxidized by molecular oxygen to yield hydrogen peroxide. The DAAO reaction has many biotechnological applications. Industrially its main use is to remove the side chain of cephalosporin c to give 7-aminocephalosporanic acid, a key intermediate for the production of semisynthetic cephalosporin antibiotics [1]. A fundamental question remains within the large class of flavoprotein oxidases that catalyse the oxidation of amino or α-hydroxy acids regarding the mechanism by which a proton and two electrons are transferred from the substrate α-carbon to the flavin N(5) position during the reductive half-reaction. The precise mechanism of substrate dehydrogenation by DAAO is widely debated, even if the crystal structures of the enzyme purified from pig kidney (pkDAAO) and of the enzyme from *Rhodotorula gracilis* (RgDAAO) (at a resolution of 2.6 Å and 1.2 Å, respectively) have been determined [2–4]. Over the years, three main but different mechanisms have been proposed for the reaction catalysed by this flavoenzyme (reviewed in [5]): (a) a direct hydride-transfer mechanism of α-hydrogen of the substrate to the N(5) position of the flavin [6]; (b) a concerted mechanism in which the α-proton abstraction is coupled with the transfer of a hydride from the amino group of the substrate [7]; and (c) a carbanion mechanism which involves the initial formation of a carbanion by subtracting the α-H of the substrate as a proton [8]. Thus, to deprotonate the α-proton, the enzyme must have some highly specific means of removing the proton and stabilizing the resulting carbanion. Hence, the presence of an enzyme base for α-proton abstraction is essential for the carbanion mechanism.

Comparing the primary sequences of the known DAAOs [9] and the active sites of *R. gracilis* and mammalian DAAO [2–4], it is evident that only three residues, among those identified in or near the active site, are conserved (namely two tyrosines and one arginine). The crystal structure of oxidized RgDAAO in complex with the quasi-substrate CF_3-D-alanine [4] revealed the mode of substrate binding (Fig. 1A). The α-carboxylic group of the D-amino acid interacts electrostatically with the γ- and ε-amino groups of R285 (at ≈2.8 Å) and it is hydrogen bonded to the hydroxyl groups of Y223 and Y238. The substrate α-amino group is hydrogen bonded symmetrically with the backbone C=O group of S335 and the active site water molecule H_2O72, while the substrate side chain is oriented toward the hydrophobic binding pocket of the active site (see Fig. 1A). R285 has been mutated to lysine, glutamine, aspartate, and alanine [10]. The perturbation of the active site in the R285 mutants modifies the precise substrate alignment: alteration of the reaction trajectory results in the large change observed in the reaction velocity. The low stability of the

Correspondence to L. Pollegioni, Dipartimento di Biologia Strutturale e Funzionale, Università degli Studi dell'Insubria via J.H. Dunant 3, 21100 Varese, Italy.
Fax: +39 332 421500, Tel.: +39 332 421506,
E-mail: loredano.pollegioni@uninsubria.it

Abbreviations: DAAO, D-amino acid oxidase; RgDAAO, *Rhodotorula gracilis* D-amino acid oxidase; pkDAAO, pig kidney D-amino acid oxidase; XO, xanthine oxidase; IP, imino pyruvic acid; EFl_{ox}, oxidized enzyme; EFl_{seq}, flavin semiquinone enzyme; EFl_{red}, reduced enzyme.

Enzymes: D-amino acid oxidase (DAAO; EC 1.4.3.3); xanthine oxidase (XO; EC 1.1.3.22).

(Received 16 May 2002, revised 8 July 2002, accepted 9 August 2002)

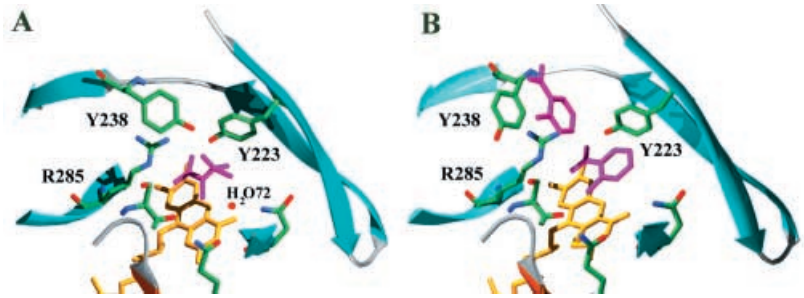

Fig. 1. Active site of *R. gracilis* DAAO in complex with (A) CF_3-D-alanine (accession code 1c0l) and (B) anthranilate (accession code 1c0i). R285, Y223 and Y238 interact in the structure of RgDAAO complexed with the substrate with the α-carboxylic group of CF_3-D-alanine [4], and are conserved in all DAAO sequences. The FAD molecule is shown in yellow and the ligand molecules in purple.

semiquinone form in the mutants prompted us to propose that, in the free enzyme form (i.e. in the absence of a ligand), the side chain of R285 is able to rotate to a distance of ~3 Å from the N(1)–C(2)=O flavin locus [10]. Mutagenesis of Y223 in RgDAAO to a phenylalanine and a serine has been completed [11]. After characterization of the corresponding mutants we were able to exclude any possibility that Y223 can act as an active-site base. The differences in properties between Y223F and Y223S mutants suggest that the side chain at position 223 contributes by fixing the substrate in the correct orientation for efficient catalysis, mainly by its shape and less by its hydrogen bonding or electrostatic properties (the aromatic ring is also important for steric reasons) [11].

For Y238 a role similar to that inferred for Y223 in binding and fixation was suggested [4]. This proposal was changed recently following the investigation of the effect of pH on benzoate binding in RgDAAO [12] and the resolution of the three-dimensional structure of RgDAAO in complex with anthranilate (PDB entry code 1c0l). The structural data show that the architecture of the active site can be modified by switching the side chain of Y238 from the position observed in the structure of DAAO in complex with D-alanine or CF_3-D-alanine (closed form) to the one adopted in the DAAO–anthranilate complex (opened form) (compare the position of Y238 in Fig. 1A with that in Fig. 1B). To obtain an insight of the role of Y238 in RgDAAO we produced and characterized two single-point mutations at site Y238 of RgDAAO.

MATERIALS AND METHODS

Reagents

Restriction enzymes and T4 DNA ligase were from Promega Life Sciences. Site-directed mutagenesis reactions were made using the Altered Sites™ II Kit (Promega Life Sciences). D-amino acids, xanthine, xanthine oxidase, and all other compounds were purchased from Sigma. Kinetic experiments were performed in 50 mM sodium pyrophosphate, pH 8.5, 1% glycerol, 0.3 mM EDTA, 0.5 mM 2-mercaptoethanol and at 25 °C; other experiments were carried out in 50 mM Hepes pH 7.5, 10% glycerol, 5 mM 2-mercaptoethanol and 0.3 mM EDTA at 15 °C, except where stated otherwise.

Site-directed mutagenesis and enzyme expression

Enzymatic DNA modifications were carried out according to the manufacturer's instructions and as described by Sambrook *et al.* [13]. The RgDAAO-Y238 mutants were generated using a dual primer method to simultaneously introduce ampicillin resistance and a site-directed mutation (Y238F: 5′-GGCGGGA*CGTTCG*GCGTGGGAG-3′, Y238S: 5′-GGCGG**GACGTC***CGG*CGTGGGAG-3′; in both cases the mutation eliminated a *Bsi*WI restriction site, shown in italics and, only for Y238S, an *Aat*II site shown in bold; the codon for the substitution is underlined). Successful mutagenesis was screened by restriction analysis and confirmed by DNA sequencing of the final plasmid. The mutant cDNAs were subcloned into the *Eco*RI restriction site of the pT7.7A (USB) expression vector (pT7-DAAO mutants). The Y238F and Y238S DAAO mutants were expressed and purified as described previously [14].

Activity assay and gel electrophoresis

DAAO activity was assayed with an oxygen electrode at pH 8.5 and 25 °C with 28 mM D-alanine as substrate at air oxygen saturation ($[O_2] = 0.253$ mM) [14]. One DAAO unit is defined as the amount of enzyme that converts 1 μmol D-alanine per min, at 25 °C. Substrate specificity was investigated by means of the same polarographic assay, using different concentrations of various D-amino acids as substrate. Analytical SDS/PAGE was carried out as described by Laemmli [15]. The expression of the mutant enzymes was also determined by Western blot analysis, using an immunostaining procedure [10,11].

Spectral and ligand binding experiments

The extinction coefficients for the mutant DAAO enzymes were determined by measuring the change in absorbance after release of the flavin. The enzymes were heat denatured by boiling for 5 min in the dark (an extinction coefficient of $11.3 \cdot mM^{-1} \cdot cm^{-1}$ at 450 nm for free FAD was used) [10,11]. Photoreduction experiments were carried out using an anaerobic cuvette containing ≈ 8 μM enzyme, 5 mM EDTA, and 0.5 μM 5-deazaflavin. The solution was made anaerobic and photoreduced with a 250-W lamp, with the cuvette immersed in a 4 °C water bath [10,16]; the progress of the reaction was followed spectrophotometrically. The thermodynamic stability of the semiquinone was determined by the addition of 5 μM benzyl viologen from a side arm of the cuvette after the photoreduction was complete. Disproportionation of the semiquinone was then followed until equilibration was reached (for up to 24 h) at 15 °C. Dissociation constants for ligands were measured spectrophotometrically at 15 °C. The change in absorbance upon adding ligand was plotted as a function of ligand concentration, after correction for any volume change.

Redox potentials

Redox potentials for the EFl_{ox}/EFl_{seq} and EFl_{seq}/EFl_{red} couples of Y238S and Y238F mutants were determined by the method of dye equilibration using xanthine/xanthine oxidase (XO) as the source of electrons [17,18]. The enzyme solution in 50 mM Hepes pH 7.5, 10% glycerol, was mixed in an anaerobic cuvette [18] with 0.2 mM xanthine, 5 μM benzyl viologen as mediator, and 1–10 μM of the appropriate dye, as reported for the wild-type enzyme [19]. The solution was purged of oxygen, and the reaction was initiated by adding 10 nM XO. The course of the reaction was followed by recording spectra at various times (typically 3–4 h), at 15 °C. Data were analysed as described by Minnaert [17]. The amount of oxidized and reduced dye was determined at a wavelength at which the enzyme has no absorbance (> 550 nm) and the amount of oxidized and reduced enzyme was determined at an isosbestic point for the dye or by subtraction of the dye's contribution in the 400–470 nm region [19]. The redox potential, E_h, for the system at equilibrium was calculated from the Nernst equation Eqn (1):

$$E_h = E_m + (2.3RT/nF) \times \log([\text{oxidized form}]/[\text{reduced form}]) \quad (1)$$

where R is the gas constant (8.31441 $V \cdot K^{-1} \cdot mol^{-1}$), T the absolute temperature, F the Faraday constant (9.6485381×10^4 $C \cdot mol^{-1}$), and n is the number of electrochemical equivalents. All the potential values are reported vs. the standard hydrogen electrode. The data were plotted according to Minnaert [17], in which the log (oxidized/semiquinone) or the log (semiquinone/reduced) couple for the enzyme is plotted vs. the log (oxidized/reduced) concentration ratio for the dye. The separation between the two single-electron transfers was estimated from the maximal percentage of the semiquinone form of the enzyme reached during a reduction experiment in the absence of the reference dye Eqns (2) and (3) [17,20]:

$$\Delta E_m = 59 \text{ mV} \times \log K \quad (2)$$

$$K = [EFl_{seq}]^2/([EFl_{red}][EFl_{ox}]) \quad (3)$$

The semiquinone formation can be determined graphically by plotting the changes in absorbance at the maximum wavelength for this form (≈ 400 nm) and for the oxidized enzyme (460 nm) and/or using the known extinction coefficient at the same wavelength [19].

Stopped-flow measurements

The experiments were performed at 25 °C in a thermostated BioLogic SFM-300 stopped-flow spectrophotometer equipped with a J & M diode array detector. The enzyme-monitored turnover method was used to assess steady-state kinetics by mixing 10 μM air-saturated enzyme with air-saturated solutions of D-alanine at 25 °C. Traces at 456 nm were analysed as described previously [10,11,21], using the KALEIDAGRAPH program (Synergy Software). For reductive half-reaction experiments, the stopped-flow instrument was made anaerobic by overnight equilibration with concentrated sodium dithionite solutions. Prior to use, the instrument was rinsed well with argon-bubbled buffer to remove the dithionite. Reaction rates were calculated by extracting traces at individual wavelengths (456 and 530 nm) and fitting them to a sum of exponentials equation using PROGRAM A (developed in the laboratory of D. P. Ballou, University of Michigan) or SPECFIT/32 (Spectrum Software Assn). PROGRAM A was also used to simulate the experimental traces using a three-step kinetic model (with only the first step reversible), in a manner analogous to that performed on wild-type DAAO [22].

RESULTS

Enzyme expression and purification

The pT7-Y238F and pT7-Y238S plasmids were used to transform BL21(DE3)pLysS *Escherichia coli* cells and the induction conditions investigated by means of Western blot analysis and DAAO activity assay. Like the wild-type RgDAAO [14], the highest level of enzyme expression and specific activity was obtained for the Y238 mutants by inducing the cells with 1.0 mM isopropyl thio-β-D-galactoside (IPTG) at saturation ($D_{600} \geq 2.0$) and cultivating them at 30 °C for an additional 1–3 h (1.6 $U \cdot mg^{-1}$ protein and 2.3 $U \cdot mg^{-1}$ protein for the Y238F and Y238S mutants, respectively). The Y238 mutants were purified to homogeneity according to the standard procedure [14]. Typically, 60–120 mg of pure enzyme was isolated from 10 L bacterial culture of Y238S and Y238F, a value close to the best expression (180 mg) obtained for wild-type DAAO [14]. The lower protein recovery of Y238 mutants compared with wild-type DAAO is due to a twofold decrease in the overall purification yield. The specific activity of the purified Y238F and Y238S preparations was ≈ 37 $U \cdot mg^{-1}$ protein (vs. 104 $U \cdot mg^{-1}$ protein for the wild-type DAAO) [14].

Spectral properties and redox potentials

The Y238 RgDAAO mutants were purified as holoenzymes (retaining their FAD prosthetic group). The mutants, in their oxidized state, show the typical spectrum of the FAD-containing flavoproteins (line 1 in Fig. 2), an extinction coefficient at 455 nm of ≈ 12 600 $\cdot M^{-1} \cdot cm^{-1}$, and a ratio $A_{274}/A_{455} \approx 8.7$. All of the Y238 mutants of RgDAAO are competent in catalysis: the anaerobic addition of an excess of D-alanine (trace 3 in Fig. 2) resulted in instantaneous enzyme reduction of all mutants, with a spectrum like that of the wild-type. Stabilization of the anionic semiquinone is typical for D-amino acid oxidases and for the family of flavoprotein oxidases [23]. The amount of semiquinone form stabilized by each mutant was determined by anaerobic photoreduction [16] until the spectrum of the flavin semiquinone (EFl_{seq}) reached a maximum (trace 2 in Fig. 2); this species represents near-complete formation of EFl_{seq} (≈ 95%) for both Y238F and Y238S (see Table 1). The maximal semiquinone formed by photoreduction is a kinetically stabilized species. Anaerobic addition of benzyl viologen resulted in dismutation of EFl_{seq} to the oxidized and reduced forms, with the endpoint containing the thermodynamically stabilized amount of semiquinone. The Y238S mutant showed a higher percentage of the thermodynamically stabilized semiquinone form than the wild-type and Y238F DAAOs (Table 1). The redox

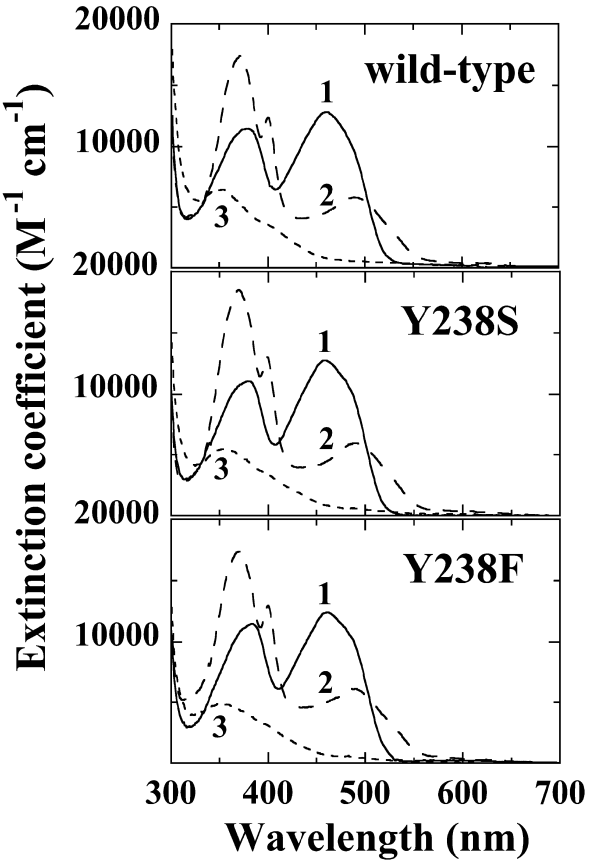

Fig. 2. Spectral properties of wild-type, Y238S, and Y238F RgDAAOs. (1) Oxidized enzyme in 50 mM Hepes buffer pH 7.5, containing 10% glycerol and 5 mM 2-mercaptoethanol, at 15 °C; (2) semiquinone form generated by photo-irradiation in the presence of 5 mM EDTA and 0.5 μM 5-deazaflavin; (3) fully reduced enzyme from the anaerobic reaction with 5 mM D-alanine.

potentials of the Y238S DAAO mutant were thus measured by the dye equilibration method of Minnaert [17], in order to assess changes in the thermodynamic properties of the flavin centre caused by the mutation and to explain the different thermodynamic stability of the semiquinone form with respect to wild-type and Y238F DAAOs. When the XO-mediated reduction of Y238S mutant was monitored in the absence of a reference dye, the percentage of semiquinone formed during the reduction was higher (80%) than that observed for the wild-type enzyme, indicating a larger separation between the single-electron potentials than in the wild-type RgDAAO [19]. The potentials of the oxidized/semiquinone and semiquinone/reduced forms of Y238S DAAO were determined by using indigo tetrasulfonate and safranine T as reference dye (data not shown). The redox potential difference with respect to the dye was calculated by plotting the log (EFl_{ox}/EFl_{seq}) or log (EFl_{seq}/EFl_{red}) flavin species of the enzyme as a function of log (oxidized/reduced) of the dye [17,19] (see Table 1). Decreasing the concentration of XO, and thus slowing the rate at which the reaction proceeds, had no effect on the potentials measured. The redox potential E_2 (= −257 mV) for Y238S DAAO is significantly more negative than the corresponding value determined for the wild-type enzyme. The ≈200 mV separation between the two single-electron transfer potentials of Y238 mutant DAAO is in agreement with the large amount of stable semiquinone form produced by photoreduction.

Benzoate is a competitive inhibitor of DAAO and in the presence of this substrate analogue the two-electron transfer is the favoured process for wild-type DAAO [19]. In order to know if the substitution of Y238 with a serine alters the redox properties even in the enzyme–substrate (or enzyme–substrate analogue) complex, the Y238S DAAO mutant was reduced in the presence of benzyl viologen of a saturating concentration of sodium benzoate (100 mM, see below) using the xanthine/XO system. For wild-type DAAO, and different from the result obtained for the free enzyme, the amount of semiquinone form produced under these experimental conditions is ≈20% [19]. When the same experiment was performed using the Y238S mutant DAAO, the spectrum of the oxidized enzyme was converted into the reduced form, lacking the isosbestic points and peak maxima characteristic of the formation of the semiquinone intermediate. The amount of semiquinone form produced in such a way for Y238S was ≈22%, corresponding to a maximal separation between the potentials for each single-electron transfer of 43 ± 14 mV (36 mV for the wild-type DAAO). This result indicates that the modification in redox properties following the substitution of Y238 with a serine residue is observed only in the free enzyme form, while the modulation of the redox properties of the Y238S DAAO by the substrate analogue binding is similar to that observed for the wild-type DAAO.

Ligand binding

Dissociation constants for several ligands were measured in order to determine the contribution of residue Y238 to

Table 1. Semiquinone formation and stabilization, and redox potentials of the free forms of wild-type and Y238 mutants of D-amino acid oxidase. The semiquinone form of DAAO was achieved by anaerobic photoreduction, and the percentage of thermodynamically stabilized form was measured after equilibration with benzyl viologen.

	Semiquinone measured (%)		E (mV)		
	Kinetically stabilized	Thermodynamically stabilized	$E_1^{\circ\prime}$	$E_2^{\circ\prime}$	E_m
Wild-type[c]	94	40	−43	−177	−109
Y238F	≥ 95	44	ND	ND	ND
Y238S	≥ 95	82	−60 ± 2.1[a]	−257 ± 5.1[b]	−160

[a,b] The redox potentials were measured at pH 7.5 and 15 °C using [a] indigo tetrasulfonate (−43 mV), [b] safranine T (−276 mV) as redox standards, and xanthine/xanthine oxidase as the source of reducing equivalents [17–19]. [c] [19].

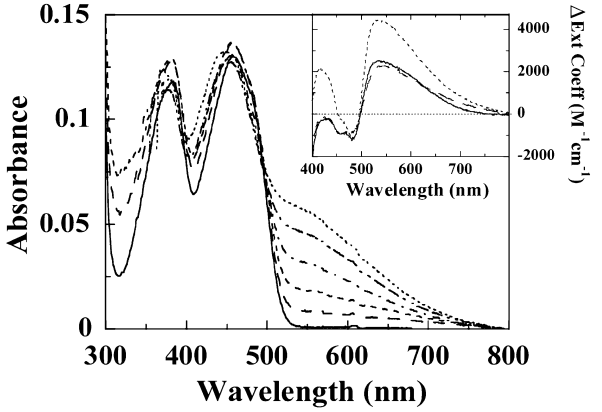

Fig. 3. Effect of anthranilate binding on the spectrum of Y238F D-amino acid oxidase. (—) ≈ 11 μM Y238F DAAO in 50 mM Hepes buffer pH 7.5, containing 10% glycerol, and 5 mM 2-mercaptoethanol; after the addition of 0.075 mM (– – –) 0.725 mM (- - -), 1.45 mM (– - –), 5.7 mM (– - - –) and 30 mM (···) anthranilate (all final concentrations), at 15 °C. Inset: difference spectra for anthranilate binding to wild-type (—), Y238F (···), and Y238S (– – –) DAAOs. The difference spectra were obtained by subtraction of the absorbance spectrum of the free oxidized form of DAAOs to the spectrum of the same enzyme after addition of a saturating concentration (≈ 20 mM) of sodium anthranilate.

substrate/ligand binding. Binding was measured by the perturbation of the visible spectrum of the FAD upon formation of the bound complex (see Fig. 3 for Y238F and anthranilate). With all the compounds tested and for both Y238 mutants, the spectral modifications were qualitatively identical to those observed for the binding to the wild-type DAAO [11,14]. Different from wild-type and Y238S, the Y238F RgDAAO mutant showed a significant increase in the intensity of the 'charge transfer' absorbance band at ≈ 600 nm following the binding of anthranilate (Fig. 3, inset) and the shoulder at ≈ 500 nm following the binding of benzoate ($\Delta\varepsilon_{497nm}$ of 7500·M^{-1}·cm^{-1} vs. a figure of 2000–4000·M^{-1}·cm^{-1} observed with the other DAAO forms) [12]. Anyway, only modest effects (less than fivefold) in binding were observed for Y238 mutants with the ligands tested (Table 2). These results indicate that the mode of ligand binding is retained in the two mutants, and that the alteration of the spectral effects can be attributed to an altered polarity of the active site. The formation of a sulfite covalent adduct to the N(5) flavin position is also marginally altered by the substitution of Y238 (Table 2).

Steady-state and rapid reaction kinetics with D-alanine

The ability of the Y238 mutants to catalyse D-alanine/oxygen catalysis was measured by enzyme-monitored turnover [21]. Air-saturated solutions of Y238 mutant enzymes and of D-alanine were mixed in the stopped-flow spectrophotometer and the absorbance spectra were recorded continuously in the 350–650 nm wavelength range at 25 °C. Following absorbance at 455 nm, an initially rapid decrease in the oxidized flavin absorption was observed, followed by a steady-state phase, and then by a further decrease to reach the final reduced state (corresponding to spectrum 3 in Fig. 2) [24]. During turnover the enzyme is

Table 2. Binding of aromatic and aliphatic competitive inhibitors and of sulfite to wild-type and Y238 mutants of D-amino acid oxidase. All measurements were made in 50 mM Hepes buffer pH 7.5, 10% glycerol, 5 mM 2-mercaptoethanol, at 15 °C. Wavelengths used to calculate the ligand binding are 497 nm for sodium benzoate and sodium crotonate, 456 nm for sodium sulfite, 540 nm for sodium anthranilate, and 345 nm and/or 380 nm for L-lactate. The K_d values were determined by plotting the change in absorbance upon adding ligand as a function of ligand concentration [32].

	K_d (mM)		
Compound	Wild-type[a]	Y238F	Y238S
Benzoate	0.9	4.4	1.1
Anthranilate	1.9	0.9	2.1
Crotonate	0.4	0.3	0.6
L-Lactate	16.2[b]	4.2	5.5
Sulfite	0.12	0.2	0.3

[a] [11]. [b] [4].

present largely in the oxidized form, indicating that the overall process of reoxidation of reduced DAAO with oxygen is always faster than the reductive half-reaction (see Fig. 4 for Y238S). The Lineweaver–Burk plots of D-alanine/oxygen turnover show a set of slightly converging lines with Y238F DAAO mutant, consistent with a ternary complex mechanism. For Y238S, as well as for wild-type DAAO [24], a parallel line pattern in the secondary plots was found instead. Such a behaviour was demonstrated to be consistent with a limiting case of a ternary complex mechanism, where some specific rate constants (i.e. k_{-2}, the reverse of the reduction rate) are sufficiently small [24]. For Y238F and Y238S, k_{cat} is reduced by about one-third (Table 3). In comparison with wild-type RgDAAO, the K_m for D-alanine is increased threefold in the mutants and the K_m for O_2 is decreased (up to 10-fold in the Y238S mutant, see Table 3).

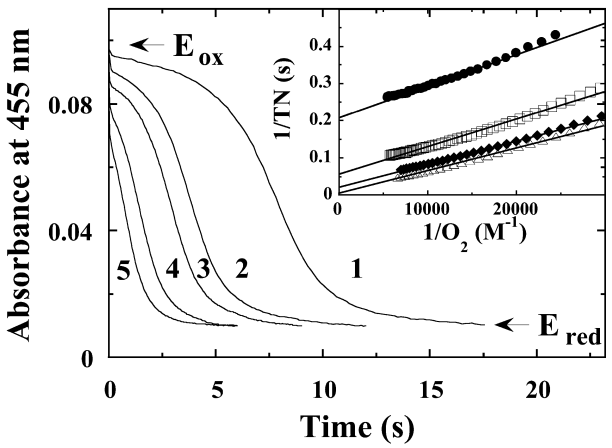

Fig. 4. Time courses of turnover of Y238S mutant RgDAAO followed in the stopped-flow spectrophotometer. The changes in absorbance were monitored at 455 nm after mixing 8.7 μM mutant enzyme with the following D-alanine concentrations: 0.5 mM (1, ●), 0.83 mM (2), 1.25 mM (3, □), 2.5 mM (4, ◆) and 5 mM (5, △). Inset: Lineweaver–Burk plot of the data determined from the enzyme monitored turnover traces depicted in the main graph.

Table 3. Comparison of the steady-state coefficients obtained from stopped-flow experiments of wild-type and Y238 mutants of D-amino acid oxidase. All measurements were made in 50 mM sodium pyrophosphate, pH 8.5, 1% glycerol, 0.3 mM EDTA and 0.5 mM 2-mercaptoethanol.

	Lineweaver–Burk plot	k_{cat} (s^{-1})	$K_{m,D\text{-Ala}}$ (mM)	K_{m,O_2} (mM)	$\Phi_{D\text{-Ala}}$ (M·s)	Φ_{O_2} (M·s)	$\Phi_{D\text{-Ala},O_2}$ (M^2·s)
Wild-type[a]	parallel	350	2.6	2.3	7.5×10^{-6}	6.7×10^{-6}	
Y238F	≈ convergent	125	7.5	0.26	5.9×10^{-5}	5.2×10^{-6}	1.1×10^{-8}
Y238S	≈ parallel	120	7.8	0.96	6.5×10^{-5}	7.9×10^{-6}	

[a] [24].

The ternary complex mechanism shown in the upper loop of Scheme 1 can be described using the conventions of Dalziel [25]:

$$e_t/v = \Phi_0 + \Phi_{D\text{-Ala}}/[D\text{-Ala}] + \Phi_{O_2}/[O_2] + \Phi_{D\text{-Ala},O_2}/[D\text{-Ala}][O_2] \quad (4)$$

where: $k_{cat} = 1/\Phi_0$; $K_{m,D\text{-Ala}} = \Phi_{D\text{-Ala}}/\Phi_0$; $K_{m,O_2} = \Phi_{O_2}/\Phi_0$

Scheme 1

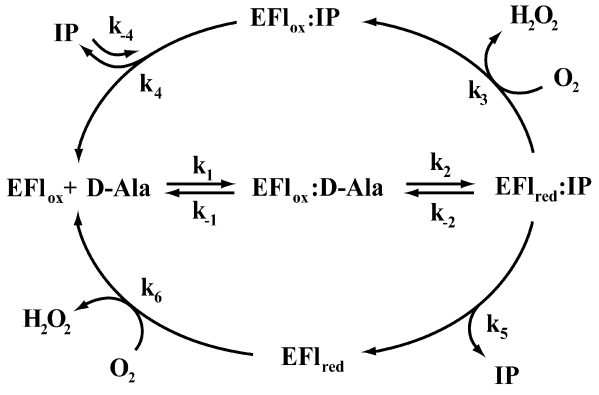

Scheme 1. Kinetic scheme of the reaction of RgDAAO with D-alanine. The upper loop shows the ternary complex mechanism, and the lower loop depicts the ping-pong mechanism. IP, imino pyruvate.

$$\frac{e_t}{v} = \frac{k_2 + k_4}{k_2 \cdot k_4} + \frac{k_{-1} + k_2}{k_1 \cdot k_2[D\text{-Ala}]} + \frac{k_2 + k_{-2}}{k_2 \cdot k_3[O_2]} + \frac{k_{-1} + k_{-2}}{k_1 \cdot k_2 \cdot k_3[D\text{-Ala}][O_2]} \quad (5)$$

The reductive half-reaction of Y238 mutants with D-alanine was measured by mixing anaerobically a solution of each mutant enzyme with solutions containing varying concentrations of D-alanine, such that a pseudo first-order condition was maintained with respect to the substrate. In the absence of oxygen, the oxidized form of each single mutant was rapidly converted to the reduced enzyme–imino pyruvate (IP) complex (phase 1, steps k_1/k_{-1} and k_2/k_{-2}), followed by decay of the spectral intermediate (phase 2, k_5/k_{-5}) [22,24]. Like the wild-type RgDAAO, no spectral change has been associated with formation of the EFl_{ox}–D-alanine complex in the reductive half-reaction of any of the Y238 mutants. As shown for Y238F in Fig. 5A, the formation of the spectral intermediate, phase 1, involved a large extinction decrease at 456 nm and a small extinction increase at 530 nm, consistent with formation of a EFl_{red}–IP charge-transfer complex [22,24]. Decay of the spectral intermediate, phase 2, resulted in a decrease in absorbance at 456 nm and 530 nm, giving a spectrum consistent with the presence of free, reduced enzyme (Fig. 5A) [24]. In the case of the Y238F mutant, the increase in absorbance at 530 nm is observable only when the production of the EFl_{red}–IP complex is fast, i.e. at high D-alanine concentrations, indicating a fast dissociation of the imino acid from the reduced enzyme form (see below). The rates of flavin reduction, k_{obs1}, for Y238F and Y238S mutants at different D-alanine concentration are close to those determined for

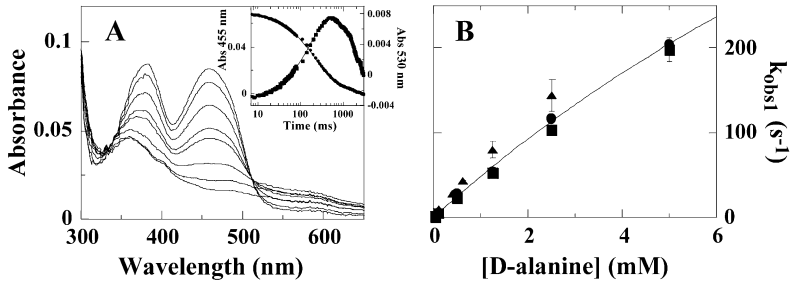

Fig. 5. (A) Spectral courses of anaerobic reduction of Y238F DAAO by D-alanine and (B) plot of the dependence of the observed first rate of anaerobic reduction (k_{obs1}) for wild-type (▲), Y238F (■), and Y238S (●) DAAOs on the concentration of D-alanine. (A) Y238F DAAO (7.5 μM) was mixed anaerobically with 0.1 mM D-alanine in the stopped-flow instrument, at pH 8.5 and 25 °C. From the top at 455 nm: spectrum at 10 ms (is essentially unreacted enzyme), 50 ms, 108 ms, 195 ms, 310 ms, 510 ms, 1.0 s and 2.24 s after mixing. Inset: time courses of flavin reduction followed at 455 nm (●) and 530 nm (■), during the same experiment depicted in the main graph. The solid traces represent fits to the data according to a two sequential exponentials equation. (B) The reaction rates were determined from experiments as those reported in (A). The line is the best fit obtained for the values determined for the Y238S DAAO mutant [26].

the wild-type DAAO (Fig. 5B). At pH 8.5, wild-type RgDAAO and Y238 mutants show a hyperbolic dependence of the observed first rate of flavin reduction as a function of D-alanine concentration (see Fig. 5B) [22]: a saturation is not visible as the reactions at D-alanine concentration > 5 mM develop so rapidly that the reaction rates are at the detection limit of the stopped-flow instrument (= 200·s^{-1}). Such a hyperbolic dependence of the observed reduction rate, as a function of D-alanine concentration, describes a first-order reaction of a binary complex, following a second-order complex formation (Scheme 1) [26]. As the data are best fit with a rectangular hyperbola that intersects the origin, these data indicate that the reduction step is essentially irreversible ($k_{-2} \approx 0$). A double reciprocal plot of these data clearly indicates a positive y-intercept (not shown). Using for the Y238 mutants the same kinetic model determined for the wild-type DAAO [22,24], k_2 and $K_{d,app}$ values were determined (Table 4). Numerically, the value of $K_{d,app}$ is equal to $(k_{-1} + k_2)/k_1$ [26], and its value is similar for the Y238 variants and wild-type DAAO. As binding never reaches equilibrium, the thermodynamic representation of substrate binding, K_d, is not nearly as important for substrate recognition as the rate of substrate association, k_1. To validate the values determined for rates > 100·s^{-1}, and to estimate lower limits for the k_1 and k_{-1} rate constants, the experimental traces at 455 nm were simulated using PROGRAM A [22]. Simulations were based on the sequential mechanism described above (i.e. a system including steps k_1, k_{-1}, k_2 and k_5, and the following extinction coefficients: EFl_{ox} and EFl_{ox}:D-Ala = 12 600·M^{-1} cm^{-1}; EFl_{red}:IP = 4600–4000·M^{-1}·cm^{-1}; EFl_{red} = 2800·M^{-1}·cm^{-1}). Good estimation of the experimental traces of Y238F and Y238S mutants at each D-alanine concentration can be obtained only using a k_1 rate constant slightly higher and a k_{-1}-value lower than the corresponding values estimated for the wild-type one; the rate of flavin reduction was instead constant for all the DAAO forms. The parameters obtained from fitting and used for simulations are listed in Table 4.

The decrease in k_{cat} for all Y238 mutants in comparison to the wild-type RgDAAO resembles the situation observed for the Y223F mutant of RgDAAO [11]. The fourfold difference between k_2 and k_{cat} could be ascribed to a decrease in k_4, the rate for IP dissociation from the reoxidized enzyme form (Scheme 1). Using the measured values of k_{cat} and k_2, a lower limit for k_4, ranging from 100 to 150 s^{-1}, can be estimated (see Eqn 5).

The second phase in reduction corresponds to k_5, a D-alanine concentration-independent rate constant, and is changed in Y238 mutants (see Table 4). The IP product dissociates more slowly from the Y238F (0.9 s^{-1}) and faster from the Y238S (8.3 s^{-1}) mutant enzyme than from the wild-type DAAO (2.8 s^{-1}). Because the rate of product release from the reduced enzyme is very much slower than k_{cat} in Y238S and Y238F (see Table 4), k_5 clearly does not lie within the catalytic cycle, and the steady-state mechanism must be essentially a ternary complex. In the case of an irreversible ($k_{-2} = 0$) ternary complex mechanism, the steady-state parameter $1/\Phi_{O_2} = k_2 \cdot k_3/(k_2 + k_{-2})$ (see Eqn 5) reduces to k_3. For wild-type DAAO, $1/\Phi_{O_2}$ is equivalent to the independently measured value of k_3, within experimental error [24]. The good correspondence between the Φ_{O_2} parameter determined with all the Y238 mutants and with wild-type DAAO (Table 3) indicates that these mutants still largely follow a ternary complex mechanism and that the oxygen reactivity (k_3) of the EFl_{red}–IP complex in the mutant is not changed.

Substrate specificity

We tested the activity of wild-type and Y238 DAAO mutants on different D-amino acids, measuring the oxygen consumption with a Clark type electrode at pH 8.5 and 25 °C [14]. The apparent kinetic parameters V_{max} and K_m for the D-amino acid determined at fixed (21%) O_2 concentration are reported in Table 5. For both Y238 mutants, and with all the substrates tested, the maximal activity was lower than the corresponding value determined for wild-type DAAO. Notwithstanding, the catalytic efficiency expressed by the V_{max}/K_m ratio is frequently similar (or slightly higher) among the mutants and the wild-type. This is due to the smaller $K_{m,app}$ values determined using the Y238 DAAO mutants for all D-amino acids tested (Table 5). The decrease in $K_{m,app}$ is evident for substrates with large, hydrophobic side chains (such as cephalosporin C and D-phenylalanine), as well as for a small and polar amino acid such as D-serine. The Y238 mutants have a similar substrate specificity to the with wild-type DAAO: the highest V_{max}/K_m ratios have been observed with D-phenylalanine and D-tryptophan. Like the wild-type DAAO, basic D-amino acids are poor substrates for Y238 mutants (data not shown). The mutants maintain the stereospecificity of the wild-type RgDAAO; they are not reduced by L-valine under anaerobic conditions.

Table 4. Kinetic parameters for the reductive half-reaction of wild-type and Y238 mutants of D-amino acid oxidase with D-alanine as substrate. The $K_{d,app}$ was obtained from the slope divided by the intercept in the double-reciprocal plot of the rate of reduction vs. D-alanine concentration. All measurements were made in 50 mM sodium pyrophosphate pH 8.5, 1% glycerol, 0.3 mM EDTA, 0.5 mM 2-mercaptoethanol. The k_1 and k_{-1} rate constants and the k_2 and k_5 values reported in parenthesis are the parameters determined by simulation of the experimental traces using program A (see text for details).

	k_2 (s^{-1})	$K_{d,app}$ (mM)	Slope ($k_2/K_{d,app}$) (M·s) × 10^{-5}	k_1 (mM^{-1}·s^{-1})	k_{-1} (s^{-1})	k_5 (s^{-1})
Wild-type[a]	510 ± 50 (500)	16 ± 3	3.0	30	500	2.3 ± 0.4 (2.8)
Y238F	= 400 (500)	11.6 ± 2.8	2.1	60	250	0.9 ± 0.2 (0.8)
Y238S	= 400 (500)	14.1 ± 3.5	2.0	40	250	8.3 ± 1.7 (10)

[a] [22].

Table 5. Substrate specificity of wild-type and Y238 mutants of D-amino acid oxidase. All measurements were made in 50 mM sodium pyrophosphate, pH 8.5, at air (21%) oxygen saturation, and at 25 °C.

	D-Alanine			D-Serine			D-Proline			D-Tryptophan			Cephalosporin C			D-Valine			D-Phenylalanine		
	V_{max} ($U \cdot mg^{-1}$)	K_m (mM)	V_{max}/K_m	V_{max} ($U \cdot mg^{-1}$)	K_m (mM)	V_{max}/K_m	V_{max} ($U \cdot mg^{-1}$)	K_m (mM)	V_{max}/K_m	V_{max} ($U \cdot mg^{-1}$)	K_m (mM)	V_{max}/K_m	V_{max} ($U \cdot mg^{-1}$)	K_m (mM)	V_{max}/K_m	V_{max} ($U \cdot mg^{-1}$)	K_m (mM)	V_{max}/K_m	V_{max} ($U \cdot mg^{-1}$)	K_m (mM)	V_{max}/K_m
Wild-type	122	0.8	152	61	13.7	4.5	116	21.5	5.4	160	0.3	530	109	5.0	21.8	195	18.9	10.3	144	0.3	480
Y238S	37.7	0.4	94	25.8	2.9	8.9	38.1	12.3	3.1	45.6	0.2	228	21.7	1.9	11.4	42.6	6.1	7.0	33.1	0.07	473
Y238F	37.4	0.4	94	40.7	1.7	24	106.1	13.5	7.9	51.4	0.3	171	11.8	1.9	6.2	62.5	6.0	10.2	27.0	0.04	675

DISCUSSION

The Y238 mutants were expressed and purified to homogeneity with a good yield using the expression system constructed to maximize the production in *E. coli* of wild-type RgDAAO [14]. The characterization of the kinetic, substrate specificity and ligand binding properties of Y238F and Y238S DAAO mutants allows us rule out a main role of the side chain of this active site residue in substrate/ligand fixation. The ligand-binding experiments demonstrate that the overall substrate-binding pocket remains intact, as all mutants bind the same ligands as the wild-type (Table 2). The steady state parameters determined with various D-amino acids at a fixed O_2 concentration (see Table 5) indicate that Y238 is not important in determining the substrate specificity of yeast DAAO. Spectral properties of the oxidized, semiquinone, and reduced forms of the Y238 mutants are essentially the same as wild-type DAAO (Fig. 2).

The first significant change observed following the substitution of Y238 concerned the flavin redox potentials of Y238S in the free enzyme form: this mutant shows a larger separation of the single-electron transfer potentials than the wild-type DAAO, thus a higher stabilization of the semiquinone form (see Table 1). The stabilization of the anionic semiquinone form depends on the protein's ability to stabilize the negative charge delocalized on the N(1)-C(2)=O flavin locus. For free RgDAAO, we previously proposed that R285 could play such a role through a conformational change [10]. The higher stabilization of the semiquinone form observed for the Y238S mutant in the free form may be the result of a better interaction of R285 with the N(1)-C(2)=O locus of the reduced flavin following the substitution of Y238 with a serine (the distance between the side chains of R285 and Y238 is 4.1 Å), or could be ascribed to an alteration of the active site polarity. Anyway, the amount of semiquinone form produced by the Y238S mutant in the presence of the competitive inhibitor sodium benzoate resembles that observed for the wild-type DAAO, thus the change in redox properties is restricted only to the free enzyme form.

The substitution of Y238 does not alter significantly the kinetic properties: the rate at which Y238 mutants are reduced by substrate is similar to that determined for the wild-type. This result clearly excludes Y238 as a possible functional group playing a role in acid/base catalysis, e.g. in the subtraction of the α-carbon proton. The most striking difference observed for the Y238 mutants in comparison to the wild-type DAAO is a decrease in the turnover number. It appears to be a decrease in k_4, the rate of product dissociation from oxidized enzyme. Other changes in kinetic properties belong to the rate constant (k_1 and k_{-1}) for substrate binding to the oxidized form, and to the k_5 rate constant for product release from the E_{red}–IP complex. All of these results point to a role of the Y238 side chain in substrate/product exchange to the active site of RgDAAO.

A superimposition of the active sites of yeast and mammalian DAAO [2–4] shows that the side chain of Y223 of RgDAAO overlaps with the position occupied by Y228 in pkDAAO (the residue located on the flexible loop that adapts its conformation depending on the size of the ligand side chain) [27] and that Y238 of RgDAAO

overlaps to Y224 of the mammalian enzyme (the residue interacting with the α-amino group of the substrate and with a buried water molecule). Y224 in pkDAAO and Y238 in RgDAAO share the characteristics of being flexible and adapting their conformation depending on the size of the ligand side chain [27]. Our results indicate that the role of Y223 and Y238 in the active site of RgDAAO is different from that of the tyrosine residues (Y224 and Y228) of pkDAAO. In fact, and different from the results obtained with RgDAAO mutants, both Y224F and Y228F mutants of pkDAAO showed a large decrease in k_{red} (30- and 100-fold lower than in the wild-type) but the $K_{d,app}$ for D-alanine was not affected significantly [28]. Furthermore, though these substitutions modified the interaction of the reduced enzyme with the IP product, as indicated by the observation that Y228F totally abolished the formation of the absorbance band centred at 560 nm during the reduction process, which is typical of the EFl_{red}–IP complex, they did not alter the rates of product dissociation [28]. Two tyrosine residues are also present at the active site of other flavoproteins, e.g. flavocytochrome b_2 [29], glycolate oxidase [30], and lactate monooxygenase [31]. It has been proposed that these enzymes work by a carbanion mechanism, and that in each enzyme these residues play a different role in fine tuning substrate interactions and enzyme activity. Their role was also investigated by site-directed mutagenesis experiments, but only by replacing a phenylalanine (a nondisruptive mutation). In the case of RgDAAO we also changed the spatial arrangement in the active site by introducing a serine.

In conclusion, the results obtained with the Y238 mutant enzymes eliminate this residue as an active site acid/base catalyst and indicate that this residue is not important for substrate/ligand fixation. Our results are in agreement with the different position of Y238 observed in the structure of DAAO in complex with D-alanine or CF_3-D-alanine (closed form) [4] with respect to that occupied in the DAAO–anthranilate complex (opened form) (Fig. 1). The movement of Y238 side chain controls substrate binding and product release, analogously to the role of the 216–228 loop present in pkDAAO [27]. The differences in properties between the Y223 and Y238 RgDAAO mutants suggest that the side chain at position 223 contributes to this by fixing the substrate in the correct orientation for efficient catalysis mainly by its shape and less by its hydrogen-bonding or electrostatic properties [11], whereas Y238 essentially controls access to the active site. These conclusions are also in agreement with the pH-dependence studies of benzoate binding [12]: for wild-type and Y238F DAAOs, the binding is pH dependent ($pK_a = 9.8$ and 9.1, respectively), whereas no change in K_d for benzoate was observed in the 5.5–10.5 pH range for the Y223F mutant. Thus, the fast release of the imino acid product observed for the Y238S DAAO can be speculatively attributed to a lower steric hindrance of the 'gate residue' in the mutant form with respect to the wild-type RgDAAO.

ACKNOWLEDGEMENTS

This work was supported by grants from Italian MIUR to Dr M.S. Pilone (PRIN 2000 Prot. MM05C73482).

REFERENCES

1. Pilone, M.S. & Pollegioni, L. (2002) D-amino acid oxidase as an industrial biocatalyst. *Biocatalysis Biotransformation* **20**, 145–159.
2. Mattevi, A., Vanoni, M.A., Todone, F., Rizzi, M., Teplyakov, A., Coda, A., Bolognesi, M. & Curti, B. (1996) Crystal structure of D-amino acid oxidase: a case of active site mirror-image convergent evolution with flavocytochrome b_2. *Proc. Natl Acad. Sci. USA* **93**, 7496–7501.
3. Mizutani, H., Miyahara, I., Hirotsu, K., Nishina, Y., Shiga, K., Setoyama, C. & Miura, R. (1996) Three-dimensional structure of porcine kidney D-amino acid oxidase at 3.0 Å resolution. *J. Biochem. (Tokyo)* **120**, 14–17.
4. Umhau, S., Pollegioni, L., Molla, G., Diederichs, K., Welte, W., Pilone, M.S. & Ghisla, S. (2000) The X-ray structure of D-amino acid oxidase at very high resolution identifies the chemical mechanism of flavin-dependent substrate dehydrogenation. *Proc. Natl Acad. Sci. USA* **97**, 12463–12468.
5. Mattevi, A., Vanoni, M.A. & Curti, B. (1997) Structure of D-amino acid oxidase: new insights from an old enzyme. *Curr. Opin. Struct. Biol.* **7**, 804–810.
6. Hersh, L.B. & Schuman Jorns, M. (1975) Use of 5-deazaFAD to study hydrogen transfer in the D-amino acid oxidase reaction. *J. Biol. Chem.* **250**, 8728–8735.
7. Miura, R. & Miyake, Y. (1988) The reaction mechanism of D-amino acid oxidase: concerted or not concerted? *Bioorg. Chem.* **16**, 97–110.
8. Walsh, C.T., Schonbrunn, A. & Abeles, R. (1971) Studies on the mechanism of action of D-amino acid oxidase. Evidence for removal of substrate α-hydrogen as a proton. *J. Biol. Chem.* **248**, 6855–6866.
9. Faotto, L., Pollegioni, L., Ceciliani, F., Ronchi, S. & Pilone, M.S. (1995) The primary structure of D-amino acid oxidase from *Rhodotorula gracilis*. *Biotechnol. Lett.* **17**, 193–198.
10. Molla, G., Porrini, D., Job, V., Motteran, L., Vegezzi, C., Campaner, S., Pilone, M.S. & Pollegioni, L. (2000) Role of arginine 285 in the active site of *Rhodotorula gracilis* D-amino acid oxidase. *J. Biol. Chem.* **275**, 24715–24721.
11. Harris, C.M., Molla, G., Pilone, M.S. & Pollegioni, L. (1999) Studies on the reaction mechanism of *Rhodotorula gracilis* D-amino acid oxidase: role of the highly conserved Tyr223 on substrate binding and catalysis. *J. Biol. Chem.* **274**, 36235–36240.
12. Pollegioni, L., Harris, C.M., Molla, G., Pilone, M.S. & Ghisla, S. (2001) Identification and role of ionizing functional groups at the active center of *Rhodotorula gracilis* D-amino acid oxidase. *FEBS Lett.* **507**, 323–326.
13. Sambrook, J., Fritsch, E.P. & Maniatis, T. (1989) *Molecular Cloning: a Laboratory Manual*, 2nd edn. Cold Spring. Harbor Laboratory Press, Cold Spring Harbor, New York.
14. Molla, G., Vegezzi, C., Pilone, M.S. & Pollegioni, L. (1998) Overexpression in *Escherichia coli* of a recombinant chimeric *Rhodotorula gracilis* D-amino acid oxidase. *Prot. Express. Purif.* **14**, 289–294.
15. Laemmli, U.K. (1970) Cleavage of structural proteins during the assembly of the head of bacteriophage T4. *Nature* **227**, 680–685.
16. Massey, V. & Hemmerich, P. (1978) Photoreduction of flavoproteins and other biological compounds catalyzed by deazaflavins. *Biochemistry* **17**, 9–16.
17. Minnaert, K. (1965) Measurement of the equilibrium constant of the reaction between Cytochrome c and Cytochrome a. *Biochim. Biophys. Acta* **110**, 42–56.
18. Massey, V. (1991) A simple method for the determination of redox potentials. In: *Flavins and Flavoproteins* (Curti, B., Ronchi, S. & Zanetti, G., eds), pp. 59–66. Walter de Gruyter, Berlin.
19. Pollegioni, L., Porrini, D., Molla, G. & Pilone, M.S. (2000) Redox potentials and their pH dependence of D-amino-acid oxidase of *Rhodotorula gracilis* and *Trigonopsis variabilis*. *Eur. J. Biochem.* **267**, 6624–6632.

20. Clark, W.M. (1960) *Oxidation-Reduction Potentials of Organic Compounds*, pp. 184–203. Williams & Wilkins, New York.
21. Gibson, Q.H., Swoboda, B.E.P. & Massey, V. (1964) Kinetics and mechanism of action of glucose oxidase. *J. Biol. Chem.* **259**, 3927–3934.
22. Harris, C.M., Pollegioni, L. & Ghisla, S. (2001) pH and kinetic isotope effects in D-amino acid oxidase catalysis. *Eur. J. Biochem.* **268**, 1–18.
23. Massey, V. & Gibson, Q.H. (1964) Role of semiquinones in flavoprotein catalysis. *Fed. Proc. USA* **23**, 18–29.
24. Pollegioni, L., Langkau, B., Tischer, W., Ghisla, S. & Pilone, M.S. (1993) Kinetic mechanism of D-amino acid oxidase from *Rhodotorula gracilis* and *Trigonopsis variabilis*. *J. Biol. Chem.* **268**, 13850–13857.
25. Dalziel, K. (1969) The interpretation of kinetic data for enzyme-catalysed reactions involving three substrates. *Biochem. J.* **114**, 547–556.
26. Strickland, S., Palmer, G. & Massey, V. (1975) Determination of dissociation constants and specific rate constants of enzyme-substrate (or protein–ligand) interactions from rapid reaction kinetic data. *J. Biol. Chem.* **250**, 4048–4052.
27. Todone, F., Vanoni, M.A., Mozzarelli, A., Bolognesi, M., Coda, A., Curti, B. & Mattevi, A. (1997) Active site plasticity in D-amino acid oxidase: a crystallographic analysis. *Biochemistry* **36**, 5853–5860.
28. Pollegioni, L., Fukui, K. & Massey, V. (1994) Studies on the kinetic mechanism of pig kidney D-amino acid oxidase by site directed mutagenesis of tyrosine 224 and tyrosine 228. *J. Biol. Chem.* **269**, 31666–31673.
29. Xia, Z.-X., Shamala, N., Bethge, P.H., Lim, L.W., Bellamy, H.D., Xuong, N.H., Lederer, F. & Mathews, F.S. (1987) Three-dimensional structure of flavocytochrome b_2 from baker's yeast at 3.0 Å resolution. *Proc. Natl Acad. Sci. USA* **84**, 2629–2633.
30. Lindqvist, Y. & Brändén, C.I. (1989) The active site of spinach glycolate oxidase. *J. Biol. Chem.* **264**, 3624–3628.
31. Müh, U., Massey, V. & Williams, C.H. Jr (1994) Lactate monooxygenase. I. Expression of the mycobacterial gene in *Escherichia coli* and site-directed mutagenesis of lysine 266. *J. Biol. Chem.* **269**, 7982–7988.
32. Stinson, R.A. & Holbrook, J.J. (1973) Equilibrium binding of nicotinamide nucleotides to lactate dehydrogenases. *Biochem. J.* **131**, 719–728.